SUPPORTING INFORMATION

Revealing Cell-Surface Intramolecular Interactions in the BlaR1 Protein of Methicillin-Resistant Staphylococcus aureus by NMR Spectroscopy

Thomas E. Frederick, Brian D. Wilson, Jooyoung Cha, Shahriar Mobashery, and Jeffrey W. Peng*

Department of Chemistry and Biochemistry, University of Notre Dame, Notre Dame, IN 46556 USA

.

*Correspondence to J.W.P. email: jpeng@nd.edu, tel: (574) 631-2983

Materials and Methods

Site-Directed Mutagenesis for Spin-labeling. For our paramagnetic relaxation enhancement experiments (vide infra), we needed $BlaR^S$ and L2short variants in which the only surface cysteines corresponded to sites for spin-label attachment. We generated these variants using the megaprimer polymerase chain reaction (PCR) approach [1]. This approach used two flanking primers and an internal primer containing the desired mutation. Two rounds of PCR were used, involving: (1) the internal primer and the flanking primer nearest the target mutation site, and (2) the second flanking primer and the megaprimer generated by the first PCR reaction. The products of each PCR were purified using a QIAquick Gel Extraction Kit prior to use in subsequent reactions. To increase the total product of the second PCR, a third PCR using the product of PCR2 as the template and the two flanking primers was performed. Double digestion was performed with NcoI and XhoI for $BlaR^S$ and SpeI and XhoI for L2short; $BlaR^S$ and L2short DNA fragments were inserted into pET28a(+) and pET41b(+) respectively.

$BlaR^S$ Expression and Purification. Apo $BlaR^S$ and cysteine variants (I531C and N548C) used in this study were produced with a pET28a(+) based expression plasmid, which coded for the water soluble C-terminal domain of BlaR1 from *S. aureu*s. Proteins for NMR studies were expressed in transformed E. *coli* BL21(DE3) bacteria grown at 37 C in Luria broth (LB)

supplemented with Kanamycin. For non-isotopically labeled protein, expression was induced at OD_{600} of 0.7 by adding IPTG (isopropyl -D-1-thiogalacto-pyranoside) and incubated at 24.1 C overnight. [U-^{15}N; U-80%-^{2}D]-BlaR^{S} was expressed according to the protocol of Marley *et al* (20). Specifically, bacteria were first cultured in a rich LB media to an OD_{600} of 0.7, transferred to 250 mL of M9 wash buffer, and subsequently transferred to D_2O M9 media containing $^{15}NH_4Cl$ and U-[^{12}C,^{1}H] D-glucose as the sole source of nitrogen and carbon, respectively. The M9 media was further supplemented with Thiamine, $MgSO_4$, and $CaCl_2$. Expression was induced with IPTG after incubating the cell suspension in media at 24.1 C for 30 minutes ($OD_{600} \approx 3.5$). Cells were harvested after 18-21 hours of expression by centrifugation at 4000 rpm for 20 minutes.

Purification proceeded as follows. The cell pellets were suspended in HEPES A buffer (20 mM HEPES, 200 mM NaCl, pH 7.5). Cell lysis was achieved using sonication. The cell lysate was centrifuged at 17,000 rpm for 20 minutes, and the supernatant was kept for further purification. The supernatant was applied to a 5 mL HiTrap SP HP column (General Electric) pre-equilibrated with HEPES A buffer. The column was washed extensively and the protein was eluted using a NaCl gradient ranging from 200-800 mM in 20 mM HEPES, pH 7.5. Protein-containing fractions were concentrated to less than 5 mL and loaded on a Sephacryl S-200 column pre-equilibrated with S200 buffer (20 mM sodium phosphate (monobasic), 150 mM NaCl, pH 7.0). For cysteine variants, S200 buffer was prepared at pH 7.4. Fractions containing BlaR^{S} were checked by SDS-PAGE and subsequently concentrated to approximately 300 µM. All purification steps were performed at 4 C.

L2short Expression and Purification. The L2 peptide sequence demonstrating the greatest aqueous solubility was GSHDLNHNINTTKPIQEFATDIHKFNWDSIDNI, which corresponded

to the C-terminal half of L2 (residues 73-105). Apo L2short and the L2short T92C variant peptide samples were produced using a GST-His6-L2short construct within a pET41b (+) expression vector transformed into BL21(DE3) cells. Expression for non-isotopically labeled and isotopically labeled peptide followed the $BlaR^S$ protocol above, with the exception that isotopic labeling was performed in H_2O based M9 media. The cell expression was harvested by centrifugation and resuspended in His A buffer (20 mM Tris Hydrochloride, 150 mM NaCl, 30 mM Imidazole, pH 7.9). The cell content was liberated by sonication; the cell lysis suspension was subsequently centrifuged at 17,000 rpm for 20 min. The resulting supernatant was loaded on a 5 mL HisTrap FF column (GE) pre-equilibrated in His A buffer. Peptide was eluted in a single step gradient to His B buffer (20 mM Tris Hydrochloride, 150 mM NaCl, 500 mM Imidazole, pH 7.9). Fractions containing protein were buffer exchanged into His A buffer and diluted to ~15 mL. Cleavage of the GST-His6-L2short construct was accomplished by the addition of 80 units of thrombin, resulting in non his-tagged L2short. The cleavage reaction was passed over the 5 mL HisTrap FF column (GE) pre-equilibrated in His A buffer. Flow-through fractions containing the peptide were concentrated to less than 5 mL and loaded on a Sephacryl S-100 column pre-equilibrated in S200 buffer. Fractions containing L2short were checked by SDS-PAGE and subsequently concentrated to 300 μM. All purification steps were performed at 4 C.

Spin-Labeling Cysteine Variants. We used two types of nitroxide spin-labels: MTSL (methanethiosulfonate) for L2short cysteine variant T92C, and IAP (iodoacetamido-PROXYL) for the $BlaR^S$ cysteine variants, I531C and N548C (see **Figure S1**). In all cases, the cysteine variants were spin-labeled according to the protocol described by Frazier *et al*. [2]. Briefly, purified cysteine variants were diluted with 20 mM sodium phosphate monobasic, 150 mM NaCl at pH 7.4 for optimal spin-labeling conditions. DTT was added to a mole ratio of 3:1 DTT:protein, and

spin-label added to a mole ratio of 10:1 spin-label:DTT. The reaction mixture was thoroughly mixed and stored at room temperature in the dark for 8-12 hours. Unreacted spin label and DTT were removed from the sample using the S-200 or S-100 columns pre-equilibrated in pH 7.0 S200 buffer for $BlaR^S$ and L2short variants respectively.

NMR Sample Preparation. All purified samples were buffer exchanged into NMR buffer (20 mM sodium phosphate dibasic, 30 mM NaCl, 0.02% NaN_3, 10% D_2O, pH 7.0) using an Amicon Ultra centrifugal filter with a 10,000 Da or 3,000 Da molecular weight cut off for $BlaR^S$ and L2short respectively. Samples containing both $BlaR^S$ and L2short were prepared by combining the two proteins 1:1 (unless otherwise noted) in dilute concentrations, and subsequently concentrated to 300 μM using a 3000 Da molecular weight cut-off Amicon Ultra centrifugal filter. Samples were loaded into Shigemi tubes except for the PRE samples; these were loaded in standard NMR tubes due to shimming issues of paramagnetic samples in Shigemi tubes [3].

NMR Assignments and Chemical Shift Perturbations. All NMR data were measured at static field strengths of 16.4 T (700.13 MHz) or 18.8 T (800.13 MHz), using Bruker Avance systems equipped with cryogenically cooled TCI probes. Backbone $^1H^N$ and ^{15}N sequential assignments followed from TROSY [4] versions of standard 3D triple-resonance experiments, including HNCA/HNCOCA, HNCACO/HNCO, and HNCACB/HNCACB [5-7]. All NMR data were processed using TOPSPIN 1.3, using SPARKY-3 [Goddard T.D., and Kneller, D.G. 2006] to aid assignments. To investigate secondary structure of the L2short construct (*vide infra*), we recorded ^{15}N-edited ^1H-^1H NOESY spectra at 18.8 T, using two mixing times, 40ms and 400ms.

To quantify chemical shift perturbations in 2-D ^{15}N-$^1H^N$ TROSY HSQC spectra, we used the formula

$$\Delta\delta_{total} = \sqrt{\left(\Delta\delta_H\right)^2 + \left(\Delta\delta_N\right)^2} \quad \text{(S1)}$$

where $\Delta\delta_H$ and $\Delta\delta_N$ are the measured $^1H^N$ and ^{15}N chemical shift perturbations, respectively. The 0.154 weight is based on the ratio from the average variances of backbone amide proton and nitrogen chemical shifts, as reported in the BMRB database [8].

^{15}N Spin Relaxation Experiments. Backbone amide ^{15}N relaxation measurements for [U-^{15}N] L2short were carried using standard 2-d pulse sequences [9,10], and included the following parameters and relaxation delays: $R_1 = 1/T_1$: 411 (twice), 658, 904, 1151, 1397, 1644, 1890, 2137, and 2466 ms; $R_2 = 1/T_2$: 8, 25, 41, 66, 82, 99, 115, 132, 148, and 157 (twice) ms with CPMG spin-locking; steady-state ^1HN-^{15}N NOE: one pair of spectra with 5 s of ^1H saturation and one pair of control spectra with no saturation, using a recycle delay of 2.5 s. Steady-state NOE (ssNOE) and R_1 data gave the heteronuclear dipolar cross-relaxation rate constant

$$\sigma_{NH} = ssNOE * R_1 * \left(\frac{\gamma_N}{\gamma_H}\right) \quad \text{(S2)}$$

For [U-^{15}N, 80% ^2D] BlaR^S, we measured backbone ^{15}N R_1 using the same pulse-scheme used for L2short, using the following relaxation delays: 48 (twice), 95, 192, 288, 400, 496, 592, 688, 800, 1040, 1200, 1343, and 1551 ms.

We used in-house non-linear least squares fitting programs to determine both relaxation rate constants and reduced spectral density values. Jackknife methods provided the uncertainties for the relaxation rate constants. For reduced spectral density mapping [11-13], we used [13],

$$\begin{aligned} J_{eff}(0) &= \frac{3}{2(3D+C)}\left(R_2 - \frac{R_1}{2} - \frac{3\sigma_{NH}}{5}\right) \\ J(\omega_N) &= \frac{1}{(3D+C)}\left(R_1 - \frac{7\sigma_{NH}}{5}\right) \qquad \text{(S3)} \\ \langle J(\omega_H)\rangle &= \frac{\sigma_{NH}}{5D} \end{aligned}$$

to extract $J_{eff}(0)$, $J(\omega_N)$, and $\langle J(\omega_H)\rangle$ from the experimental R_1, R_2, and the heteronuclear dipolar cross-relaxation rate constants. The C and D constants in **eq S3** reflect the ^{15}N chemical-shift-anisotropy and ^{15}N-^{1}H dipolar relaxation mechanisms, respectively, where $C = \Delta^2\omega_N^2/3$ and $D = \hbar^2\gamma_H^2\gamma_N^2/\langle r_{NH}^6\rangle$ The subscript 'eff' for $J_{eff}(0)$ denotes "effective", and reminds us that $J_{eff}(0)$ can harbor additional contributions from slower μs-ms exchange dynamics that modulate the ^{15}N chemical shift and broaden the resonances (cross-peaks) [13]. Monte Carlo simulations provided the uncertainties of the reduced spectral density values based on the relaxation rate constant uncertainties.

To estimate the L2short K_d from the L2short backbone ^{15}N data, we assumed the observed rate constants in the presence of $BlaR^S$ were given by the fast-exchange expression

$$R_{1,measured} = p_B R_{1,bound} + (1 - p_B) R_{1,free} \quad . \text{(S4)}$$

$R_{1,free}$ and $R_{1,bound}$ are values from isolated [U-^{15}N] L2short and [U-^{15}N, 80% ^{2}D] $BlaR^S$. We solved for p_B and then K_d using the fact that the total protein and L2short concentrations were 300 μM. The final quoted value, $K_d = 1.3 \pm 0.4$ mM, was the average and rmsd over 17 calculated K_d values, which included only NHs lacking high amplitude fast internal motions (i.e. those lacking anomalously small $J(\omega_N)$ or large $\langle J(\omega_H)\rangle$).

Paramagnetic Relaxation Enhancement Measurements. Paramagnetic relaxation enhancement (PRE) refers to the increased spin relaxation rate of a nuclear spin, due to magnetic dipole-dipole interactions with a proximal unpaired electron. In this study, we focused on the

PRE of amide proton nuclei ($^1H^N$). The PRE rates, denoted by Γ_2, were taken as the difference between the apparent R_2 of amide protons, $R_2(^1H^N)$, in paramagnetic versus diamagnetic samples,

$$\Gamma_2 = R_{2,PARA}\left(^1H^N\right) - R_{2,DIA}\left(^1H^N\right) \quad \text{(S5)}$$

Under the assumption of rigid, isotropic tumbling of the inter-spin vector, Γ_2 can be expressed as [14,15]

$$\Gamma_2 = \frac{\left(\gamma_H g \mu_B\right)^2 S(S+1)}{15 r^6}\left\{4\tau_c + \frac{3\tau_c}{1+\left(\omega_H \tau_c\right)^2}\right\} \quad \text{(S6)}$$

, where τ_c reflects both the overall rotational correlation time of the molecular harboring the amide proton, τ_{rot}, and the effective relaxation time of the electron, τ_{elec}, via [15]

$$\frac{1}{\tau_c} = \frac{1}{\tau_{rot}} + \frac{1}{\tau_{elec}} \quad \text{(S7)}$$

The $R_2(^1H^N)$ values were measured using the pulse sequence from Iwahara *et al.*[3] with relaxation delays of 4 (twice), 6, 8, 10, 12, 15, 20, 25, and 30 ms.

HADDOCK Docking of L2short to BlaR^S. A tentative model for the L2short/BlaR^S interaction was solved using the HADDOCK Expert software, using chain B of PDB 3Q7V and a helix model for residues 87-104 of L2short. Active residues for BlaR^S were defined as those residues close to the β5-β6 turn that demonstrated chemical shift perturbations greater than four standard deviations of the trimmed mean (E477, I531, V532, G534, K535, N537, N538, G565, K566). Active residues for L2short were defined as those residues showing the local maxima in the $^1H^N$-Γ_2 rates from the IAP labeled BlaR^S I531C sample (T92, D93, K96, W99, D100, D103). Passive residues were automatically defined as those surface residues directly adjacent to the defined active residues.

$$\Gamma_{2,measured} = p_B \Gamma_{2,bound} + \left(1 - p_B\right)\Gamma_{2,free} \quad \text{(S8)}$$

Here, p_B is defined as the bound population; we determined this to be 0.165, based on the K_d = 1.3 mM from the L2short ^{15}N R_1 measurements (vide supra). We further assumed $\Gamma_{2,free}$ is negligible to due to a large inter-spin distance r; hence, $\Gamma_{2,bound} \approx \Gamma_{2,measured} / p_B$. Distance restraints were calculated based on equation S6 following Battiste and Wagner [16], and included upper and lower bounds of ± 3 Å to account for errors in the K_d estimate and the measured $^1H^N$-Γ_2 rates.

References

(1) Sarkar, G.; Sommer, S. S. *Biotechniques* **1990**, *8*, 404.

(2) Frazier, A. A.; Wisner, M. A.; Malmberg, N. J.; Victor, K. G.; Fanucci, G. E.; Nalefski, E. A.; Falke, J. J.; Cafiso, D. S. *Biochemistry* **2002**, *41*, 6282.

(3) Iwahara, J.; Tang, C.; Clore, G. M. *J Magn Reson* **2007**, *184*, 185.

(4) Pervushin, K.; Riek, R.; Wider, G.; Wuthrich, K. *Proc Natl Acad Sci U S A* **1997**, *94*, 12366.

(5) Ikura, M.; Kay, L. E.; Bax, A. *Biochemistry* **1990**, *29*, 4659.

(6) Salzmann, M.; Pervushin, K.; Wider, G.; Senn, H.; Wuthrich, K. *Proc Natl Acad Sci U S A* **1998**, *95*, 13585.

(7) Salzmann, M.; Pervushin, K.; Wider, G.; Senn, H.; Wuthrich, K. *J Biomol NMR* **1999**, *14*, 85.

(8) Mulder, F. A.; Schipper, D.; Bott, R.; Boelens, R. *J Mol Biol* **1999**, *292*, 111.

(9) Dayie, K. T.; Wagner, G. *J. Magn. Reson. A* **1994**, *111*, 121.

(10) Lakomek, N. A.; Ying, J.; Bax, A. *J Biomol NMR* **2012**, *53*, 209.

(11) Farrow, N. A.; Zhang, O.; Szabo, A.; Torchia, D. A.; Kay, L. E. *J Biomol NMR* **1995**, *6*, 153.

(12) Ishima, R.; Nagayama, K. *Biochemistry* **1995**, *34*, 3162.

(13) Peng, J. W.; Wagner, G. *Biochemistry* **1995**, *34*, 16733.

(14) Solomon, I. *Phys Rev* **1955**, *99*, 559.

(15) Bloembergen, N.; Morgan, L. O. *J Chem Phys* **1961**, *34*, 842.

(16) Battiste, J. L.; Wagner, G. *Biochemistry* **2000**, *39*, 5355.

SUPPLEMENTARY FIGURES

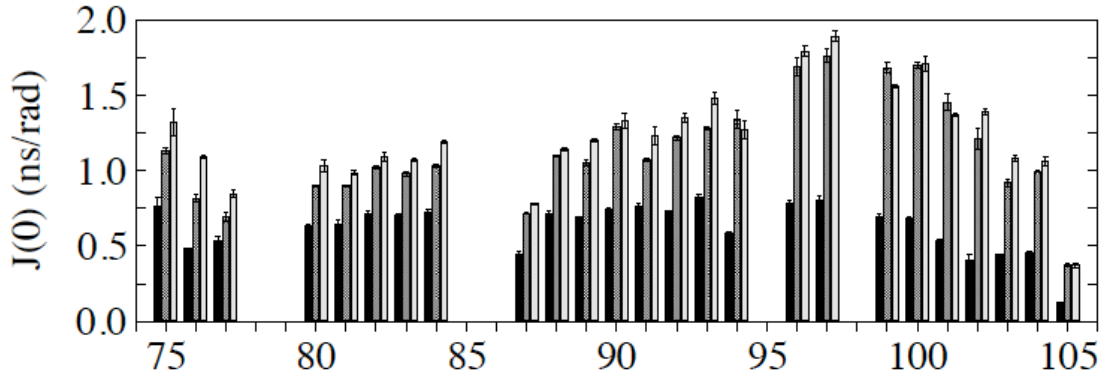

Figure S1. Reduced spectral density $J_{eff}(0)$ values for the backbone ^{15}N-^{1}H bonds of L2short in isolation (black), with unacylated BlaRS (gray), and with penicillin-G-acylated $BlaR^{S}$ (clear).

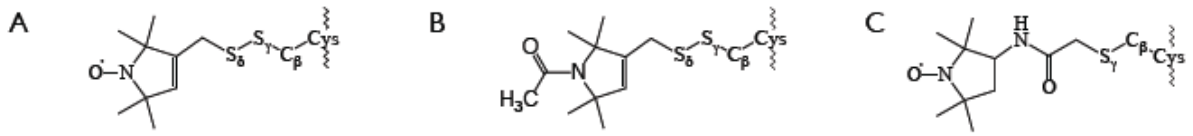

Figure S2. Paramagnetic Spin-Labels. (**A**) MTSL, (**B**) acetyl-MTSL, and (**C**) IAP. The Sγ is the intrinsic Sγ of the Cysteine residue.

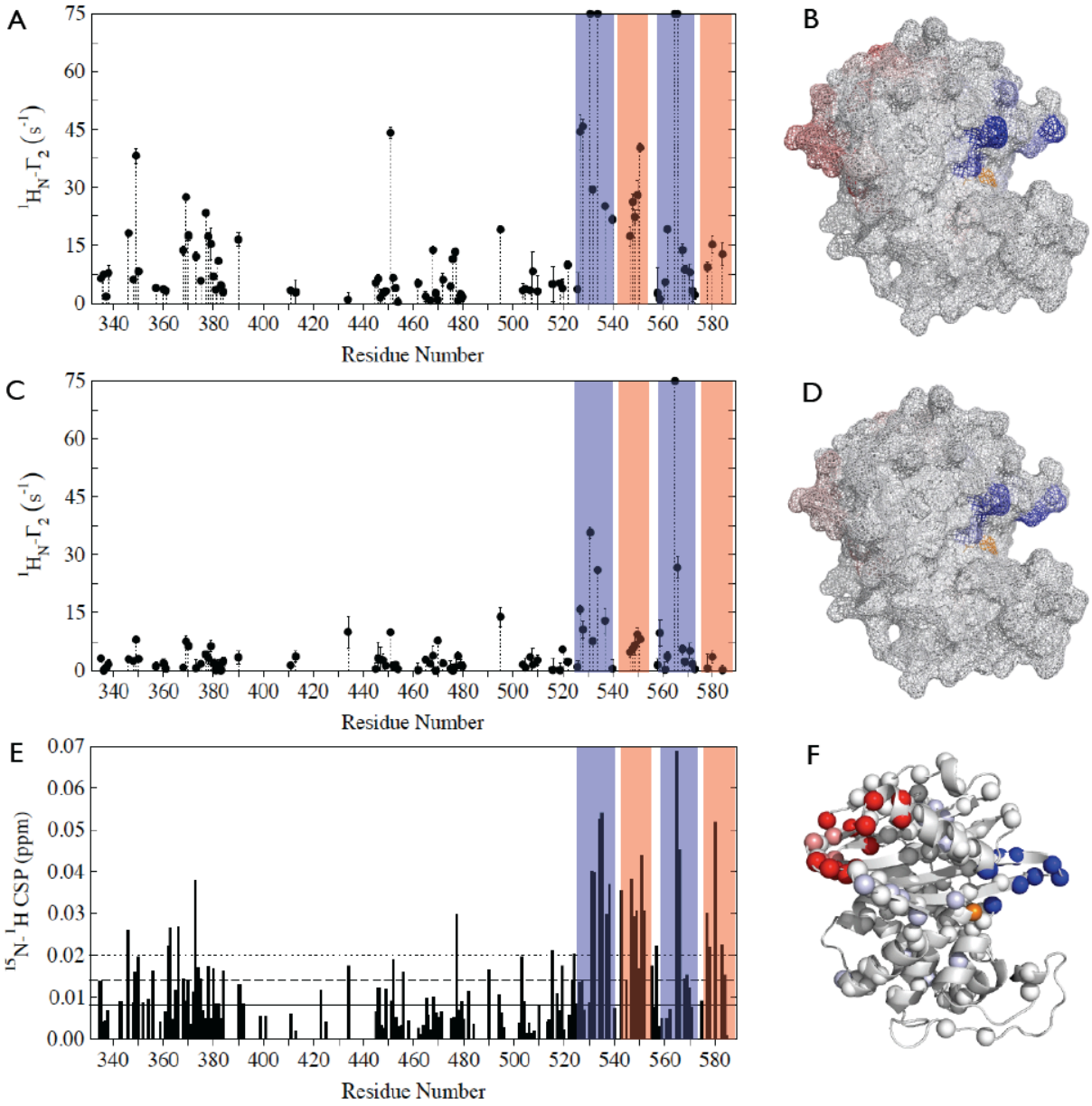

Figure S3. *Location of the L2short-BlaR^S Interaction* – (A) The measured ^1H_N-Γ_2 rates for (acetyl)-MTSL labeled L2short T92C and 80% deuterated U-[^{15}N]-labeled BlaR^S in standard NMR buffer (30 mM NaCl). Residues whose ^1H_N-Γ_2 rates could not be accurately measured due to extensive broadening were plotted as 75 s^{-1}. (B) The ^1H_N-Γ_2 rates plotted on a surface mesh rendering of the BlaR^S crystal structure (PDB 3Q7V, chain B), with blue and red indicating the different sites of interaction and shaded light to dark according to increasing ^1H_N-Γ_2 rates. (C)

The measured $^{1}H_{N}$-Γ_2 rates for (acetyl)-MTSL labeled L2short T92C and 80% deuterated U-[^{15}N]-labeled BlaR^{S} in high salt NMR buffer (150 mM NaCl). Residues whose $^{1}H_{N}$-Γ_2 rates could not be accurately measured due to extensive broadening were plotted as 75 s^{-1}. (D) The $^{1}H_{N}$-Γ_2 rates for the high salt sample plotted on a surface mesh rendering of the BlaR^{S} crystal structure (PDB 3Q7V, chain B), with blue and red indicating the different sites of interaction and shaded light to dark according to increasing $^{1}H_{N}$-Γ_2 rates. For the PREs (B/D) blue (b5-b6 turn) and red (b6-b7 turn) indicate the two L2short interaction regions. Darker shading indicates larger $^{1}H^{N}$-G_2. (E) The measured CSPs for 1:10 BlaR^{S}:L2short. The trimmed mean (black line), two standard deviations from the trimmed mean (dashed line), and four standard deviations from the trimmed mean (dotted line) are plotted for reference. (F) CSPs for residues greater than two standard deviations (light red/blue) and four standard deviations (dark red/blue) of the trimmed mean are plotted on the ribbon rendered BlaR^{S} crystal structure. For both PREs and CSPs, the antibiotic-binding-site residue S389 is in orange.

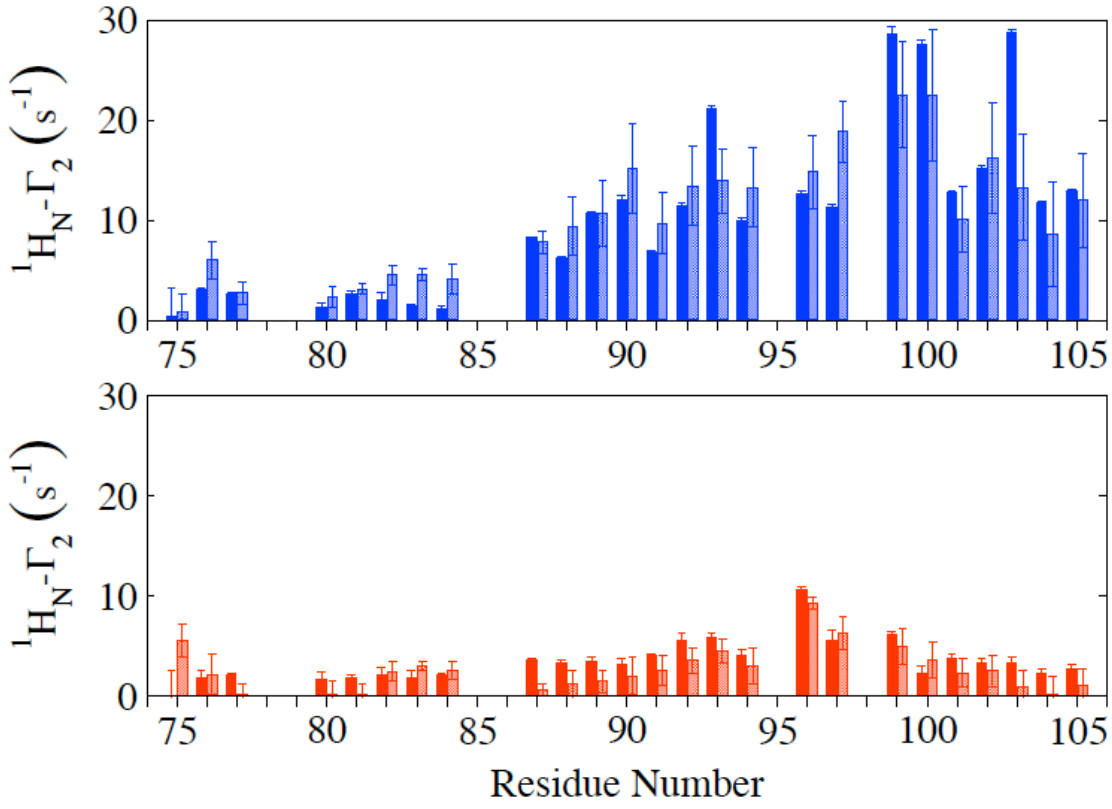

Figure S4. The $^1H^N$ rates for (A) IAP-labeled $BlaR^S$ I531C and [U- ^{15}N]-L2short without (blue) and with (light blue) penG, and (B) IAP-labeled $BlaR^S$ N548C and [U-^{15}N]-L2short without (red) and with (light red) penG.

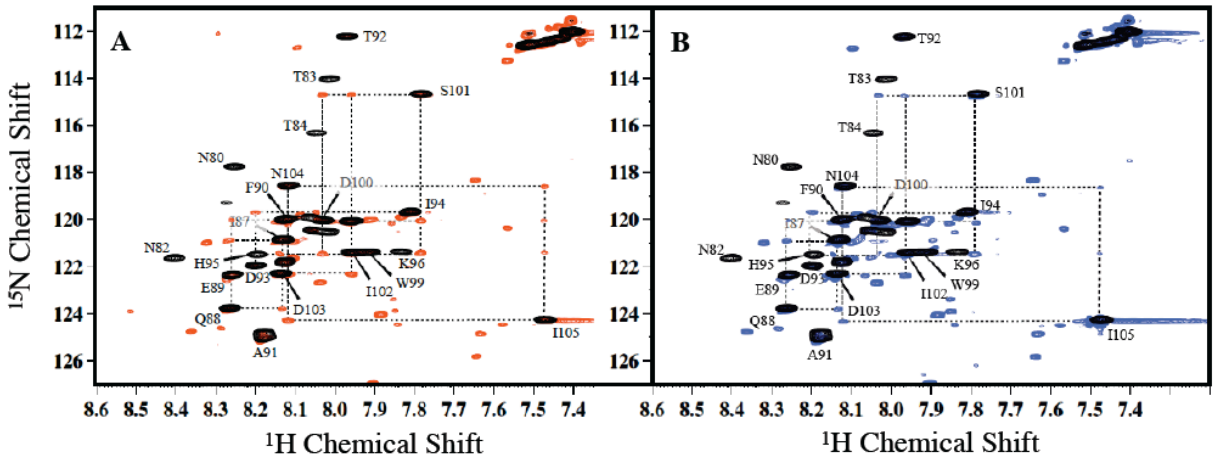

Figure S5. NOE-walk For L2short Demonstrates Helical Structure. (**A**) ^{15}N-^{1}H HSQC spectrum of [U-^{15}N]-L2short in the presence of BlaR^{S} (black) is overlaid on an ^{15}N-^{1}H HSQC-NOESY using a 400 ms NOE mixing time (red). Select residue assignments are shown, and dotted lines indicate sequential *i* to *i*+1 ^{1}H^{N}-NOEs. (**B**) Same comparison for the isolated L2short peptide. HSQC spectrum of [U-^{15}N]-L2short in the presence of BlaR^{S} (black) is overlaid on an ^{15}N-^{1}H HSQC-NOESY using a 400 ms mixing time (blue).

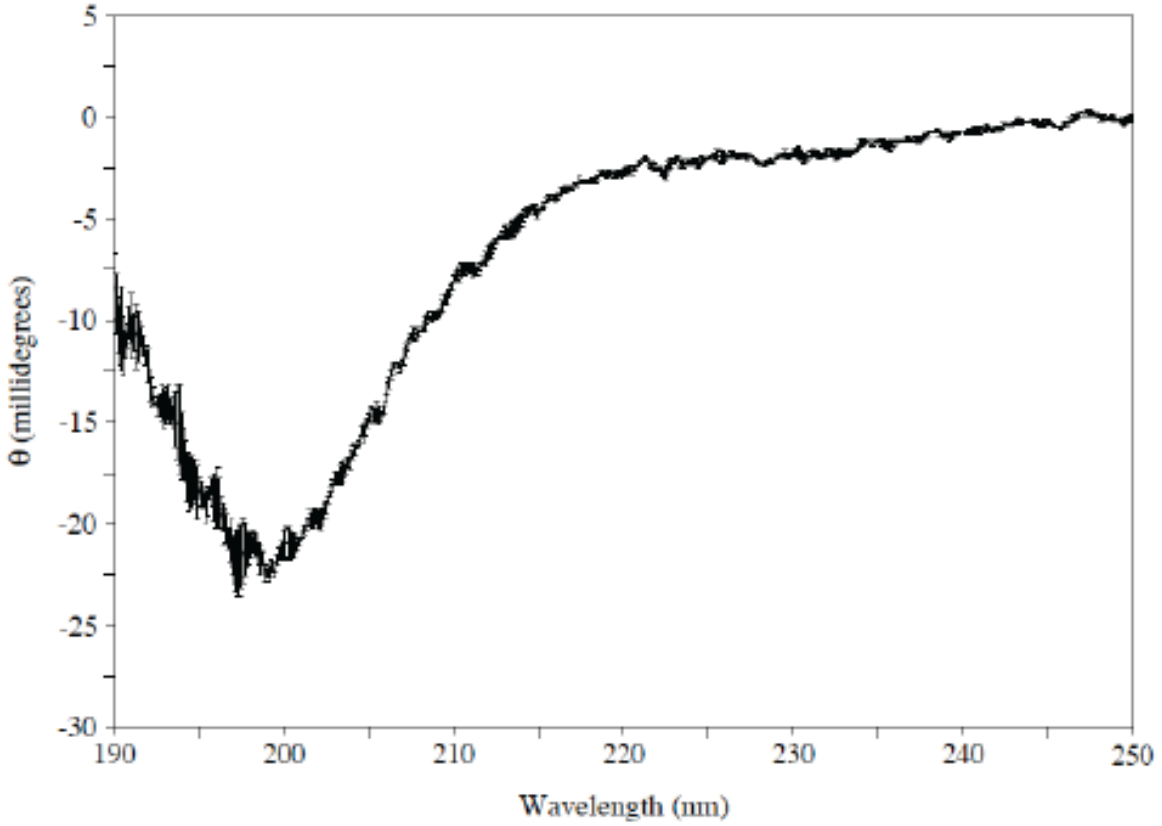

Figure S6. Far-UV CD wave scan of isolated L2short at 20 ^{0}C. The minimum near 200 nm indicates L2short is primarily random coil.